Folded Acoustic Phonons Studies in Si/Ge_xSi_{1-x} and Ge/Ge_xSi_{1-x} Superlattices

V. Lemos
Instituto de Física Gleb Wataghin, Universidade Estadual de Campinas
Caixa Postal 6165, 13083-970 Campinas, SP, Brasil

O. Pilla, M. Montagna, P. Benassi and A. Fontana
Dipartimento di Fisica, Università degli Studi di Trento
38050 Povo (Trento), Italy

C. F. de Souza and W. Carvalho Jr.
Centro de Pesquisas e Desenvolvimento, Telecomunicações Brasileiras S.A
13081 - Campinas, SP, Brasil

Received July 12, 1993

Raman scattering from folded acoustic phonons is proposed as an alternative method to x-ray diffractometry for structural characterization of superlattices. A comparison between results obtained from both kind of measurements for the same set of samples is presented. The excellent agreement confirms the reliability on determinations of the period of superlattices through high resolutioii Raman scattering. We also report the observation of spectra from highly absorbing Ge-based superlattices, which display peculiar lineshapes.

I. Introduction

It has been realized over the past few years that structural parameters estimated from the growtn conditions are often inaccurate. Analysis of structural properties by x-ray diffraction. foi instance. reveals deviation often approaching 15% of quoted values. either on the period or layer thicknesses, thus pointing to the need for a previous characterization. The possibility to use results oil high resolution Raman scattering from folded acoustic phonons for structural characterization was suggested in a more general review of Raman spectroscopy,[1] but a systematic comparison between results from x ray diffraction and Raman scattering is still lacking. Several aspects of the superlattice folding effect. can be found in ref. 2.

Here, we describe results of high resolution Raman scattering on Si/Ge_xSi_{1-x} superlattices and we demonstrate the usefulness of these results as an alternative method for structural characterization. The method is interesting because: (i) visihle light is not hazardous as x-ray can be; (ii) the mathematical simplicity of the available equation for the dispersion curves enables rapid calculation of the superlattice period and intensity analysis allows for the inner structure determination; (iii) it is convenient in case where an x ray system is difficult to set up, as in high vacuum chambers. The method is particularly suitable for thick layers superlattices for which conventional Raman scattering fails to probe the frequency region for acoustic phonons occurring very close to the laser line. A series of Si/Ge_xSi_{1-x} superlattices with varying periodicity and germanium compositions were selected as samples. Comparison with double crystal x-ray diffraction results for a chosen sample is furnished in order to demonstrate the reliability of the technique proposed here.

We also report the observation of acoustic phonon spectra in Ge/Ge_xSi_{1-x} superlattices, grown on Ge

substrate. These superlattices yield broacler structures in the spectra tlian tliose observed for the Si/Ge_xSi_{1-x} superlattices on Si substrate. The most striking structures in the spectra are the dips that occur among these broad structures. These dips are tentatively attributed to phonon-coupling effects.

II. Experimental

A new Double-monochromator SOPRA, especially designed fo. low-frequency light scattering studies, was used in our measurements.[3] The incoming beam pass twice in each monochromator via. two pairs of intermediate mirrors. When using the 514.5 nm wavelength, if the incidence angle is close to the blaze angle, this instrument works at the 11^{th} order of that line, yielding a free spectral range of about 2 000 cm^{-1}. In this configuration, tlie so called Double-Monochomator Double Pass, DMDP, is set for its highest resolution performance (giving 0.024 cm^{-1} with slit widths of 20 μm). Because extreine resolution was not needed in our measurements, we removed the two pairs of intermediate mirrors to increase transmittance. This setting allowed resolution of 0.23 cm^{-1} (0.46 cm^{-1}) with slit width of 200 μm (300 μm), employed here for Ge-based (Si-based) samples. Tlie experimental set-up is described elsewhere.[3] The Raman scattering measurements were carried out using a 90^o scattering geometry, which is nearly backscattering inside tlie sample.[4] Tlie excitation was tlie 514.5 nm line of an Ar^+ ion laser with 310 mW of output power. The incident light was polarized in tlie plane of incidence, and the polarization of the scattered light was not analysed. Our samples were grown by molecular beam epitaxy on (001) oriented surfaces.[5] The structure consisted of Si/Ge_xSi_{1-x} multi-layers deposited on Si-substrate or Ge/Ge_xSi_{1-x} on Ge-substrate of various thicknesses and composition. Their characteristics are listed in Table I. We also list in Table I, the sampling depth for the line used in these experiments (514.5 nm). These values indicate that only the multilayer structures are probed ill our measurements.

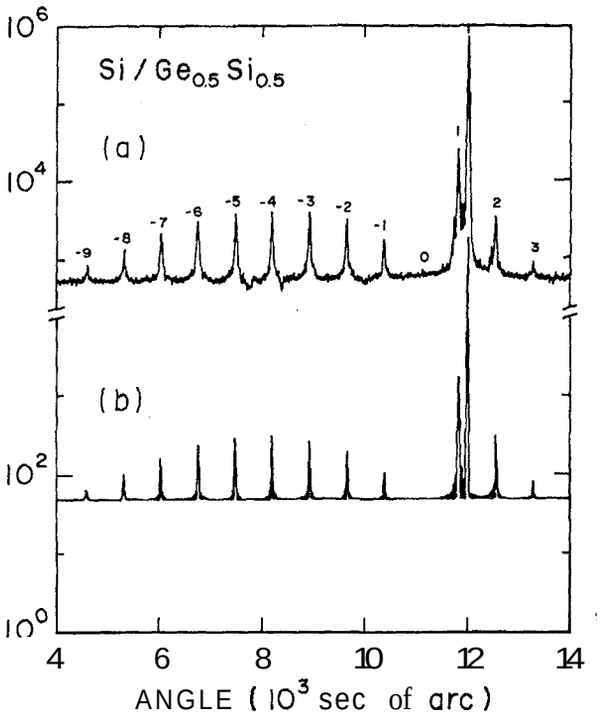

Figure 1: (a) Rocking curves (sample 2) and (b) calculated profile.

III. Results and discussion

a) x-ray diffraction

Tlie usual method to deduce structural parameters of superlattices is x-ray diffraction. Rocking curves give the period of a superlattice, d , by measuring the spacing AO between satellite peaks. The equation relating tliese quantities follows from maxima in the diffracted amplitude:[6]

$$d = \frac{\lambda \mid \gamma_H \mid}{\Delta\Theta \sin 2\Theta_B} \qquad (1)$$

Here, γ_H are the direction cosines of diffracted waves, λ is the x-ray wavelength, and Θ_B is the Bragg angle of the substrate. The order of diffraction was omitted for the salte of simplicity.

Double-crystal x-ray diffraction measurements were carried out using a Cu-K, (400) reflection. Fig. 1(a) shows experimental rocking-curves for sample 2 described in Tahle I. The substrate gives rise to the sharpest line in the spectruin. In addition, nine satellite lines of the superlattice are clearly visible. Their spacing yielcled the average superlattice period thickness listed in Table II. The values for Ge coinposition,

Table 1: Data for Si/Ge_xSi_{1-x} superlattices. Ge molar fraction in the alloy, x, pure-Si/alloy thickness ratio, d_1/d_2, period, d, total alloy thickness, nd_2 and sampling depth, D (all of these samples have 20 periods).

Sample	x	d_1/d_2	d (Å)	nd_2 (Å)	D (Å)
1	0.4	3.33	325	1500	928
2	0.5	4.54	305	1100	751
3	0.6	5.0	270	900	631
4	0.6	7.5	255	600	631

x, and the ratio d_2/d were obtained by numerical simulation of tlie diffraction spectrum.[6] It was assumed in this calculation tliat the lattice mismatch was entirely accommodated as strain ill tlie alloy layers, owing to tlie fact tliat this type of superlattice grows commensurate with the substrate. Tlie result of this simulation is sliown in Fig. 1(b). Tlie values obtained by this procedure were: x = 0.44 and $d_2/d = 0.192$. Tliese values served the purposes of defining a procedure to interpret our Raman spectra, as described further on.

b) Raman scattering

The validity of the elastic model for light scattering by acoustic phonons was confirmed in previous studies of Si/Ge_xSi_{1-x} superlattices[7-9], as well as other systems.[1] The dispersion relation predicted by tliis model, tlie Rytov's equation, reads:[10]

$$\cos(qd) = \cos\left(\frac{\omega d_1}{v_1} + \frac{\omega d_2}{v_2}\right) - \frac{\varepsilon^2}{2} sin\left(\frac{\omega d_1}{v_1}\right) sin\left(\frac{\omega d_2}{v_2}\right) \quad (2)$$

In this equation, q is the superlattice wavevector along tlie growth direction and ω tlic frequency of the folded acoustic phonons. Tlic parameters d_1 and d_2 stand for the pure-element and alloy layer thicknesses, respectively. Keeping tlie convention of subindex as before, v_1 and v_2 are tlie sound velocities and ρ_1 and ρ_2 the densities. The term,

$$\epsilon^2 = \frac{(\rho_2 v_2 - \rho_1 v_1)^2}{\rho_2 v_2 \rho_1 v_1} \quad (3)$$

describes the acoustic modulation through the relative difference between the acoustic impedances $\rho_i v_i$ of both bulk constituents.

Tliis model was adopted for analysing our measured frequencies. Assuming all pararneters in eq.(2) would be a sluggish task. Certain simplifying assumptions based on observed trends were made. For instance, tlie FLA frequencies were observed to be highly sensitive to our choice of v_1 and d but not strongly dependent on the choice of d_1/d_2. Therefore this ratio was then taken as constant, throughout our calculations. We used fixed values: $\rho_{Si} = 2.33$ g/cm^3 and $\rho_{Ge} = 5.36$ g/cm^3 and a linear interpolation of tliese two for tlie Ge_xSi_{1-x} alloys. The optical constants were taken from ref. 11. Sound velocities for Ge were tlie values $v^L_{Ge} = 4.91$ x 10^5 cm/s for longitudinal and $v^T_{Ge} = 3.54$ x 10^5 cm/s for transversal waves.[12] This left either d or v_1 as parameters. The need to use adjusted values of some bulk parameters was demonstrated in ref. 8, where four parameters were employed to match the experimental dispersion curves. In order to deduce the value of v_1 we used the x-ray diffraction data described above to fit the Folded Longitudinal Acoustic, FLA, dispersion curves for one of the samples. The result was used to analyse the Raman scattering of all of the remaining samples, to determine their period thicknesses.

The Raman scattering measurements for the Si-based superlattices were performed with incident polarization ill tlie plane of scattering thus probing only the A_1 symmetry.[4] Fig. 2 shows the high resolution Raman spectrum obtained for the $Si/Ge_{0.5}Si_{0.5}$ superlattice (sample 2). In this figure, the folded longitudinal acoustic phonons appear as well resolved lines (marlred by arrows) up to the fourth order of folding. In spite of tlie scattered momentum being close to the limiting wavevector, $q_{mz} = \pi/d$, it is still inside the minizone. Tlierefore, the sequence of lines is labeled according to the order of folding, m = ± 1, ± 2, ... The zero-order peak corresponds to the Brillouin mode of the superlattice. These frequencies, together with eq. (2) yielded $v_1 = 8.2$ x 10^5 cm/s. The result of the corre-

Table 2: Physical parameters for the Si/Ge_xSi_{1-x} superlattices. Refractive index, n, and reduced wavevectors, q/q_{mz} at $\lambda = 514.5$ nm. The period, d, resulted from Raman scattering, except for sample 2 (see text).

Sample	n	q/q_{mz}	ρ_2 (g/cm^3)	v_2^L 10^5 cm/s	v_2^T 10^5 cm/s	d (Å)
1	4.407	1.13	3.54	6.88	4.78	335
2	4.433	0.90	3.85	6.62	4.69	266
3	4.341	0.78	4.15	6.23	4.36	233
4	4.369	0.85	4.15	6.23	4.36	252

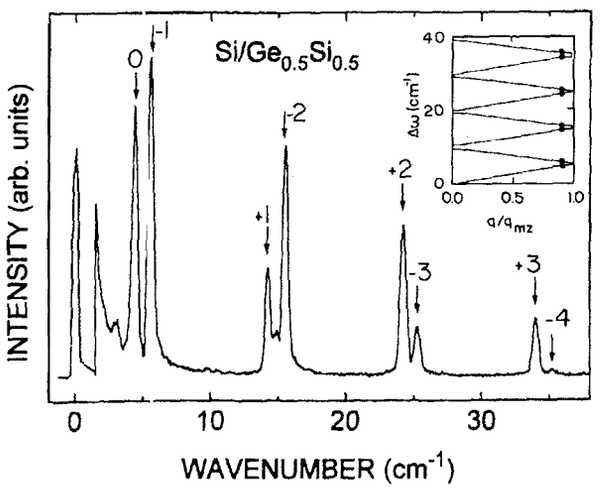

Figure 2: Rairian spectrum from FLA (sample 2) using $\lambda = 514.5$ nm.

spondent fitting is shown in the inset of Fig. 2. The agreement between calculated and observed frequencies is excellent.

Weak lines in the spectrum of Fig. 2 were interpreted as scattering by transversal acoustic phonons. Although in the experimental geometry of this work they are forhidden, a small near-forward component allows for weak, but still observable intensities. Their identification as Folded Transversal Acoustic, FTA, modes relied on fittings of the data to eq. (2). In this case, the period was kept fixed at the value $d = 266$ Å leaving v_1^T as adjustable. The value for this parameter that produccd the best fit was $= 5.5 \times 10^5$ cm/s. Finally there is one unidentified structure in the spectrum of Fie;. 2, at $\omega = 14.9$ cm^{-1}. It does not correspond to any of the FTA or FLA frequencies. It could arise from scattering due to a minizone edge longitudinal phonon, but the mechanism inducing the appearance of this particular frequency, and no other one regardless of the branch, is not clear to us.

The Raman spectruin of sample 1 is displayed in Fig. 3. For tliis sample the scattered wavevector falls outside the minizone, with $q/q_{mz} > 1$. This fulfills tlie umklapp condition for photon wavevector folding process.[4] Consequently, the ordering of the peaks appearing in the spectrum is changed. The new sequence is shown by tlie labeling of tlie lines in Fig. 3. The inset of Fig. 3 shows the fitting to ey. (2) of the experimental results for sample 1. The data of Table I, served as input, besides the value for v_1 that was taken the same as before. The fitting resulted in the value of d listed in Table II. The agreement between prediction and experimental dispersion relation is very good. Two other samples analysed in an entirely similar fashion (not shown) yielded the results listed in Table II.

Examination of FTA frequencies for all of the Si-based samples of this study produce good fitting for quite closc values of tlie parameter v_1^T. This gives an indication of the independence of the choice of v_1^T on the details of the structure.

To evaluate the reliability of our method, we performed a. fast-scan double-crystal x-ray measurement in sample 1. The value d = 333.4 Å resulted by application of eq. (1). The difference of 1.6 Å between this value and that listed in Table 11 is of the order of magnitude of one monolayer. Considering the interface roughness of about 2 monolayers usually found for

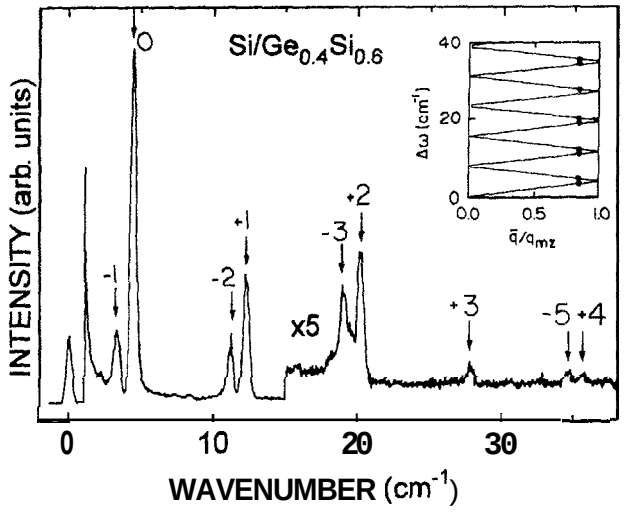

Figure 3: Umklapp assisted Raman scattering from sample 1. Inset shows the dispersioii curves.

MBE growth, the agreement between tliese two determinations of d is excellent. Tlie elastic model also predicts opening of gaps in tlie dispersion curves at zone-center and edge. Tlie magnitude of tliese gaps displays an oscillatory behavior a.s a. function of d_2/d.[13] So, ill principle, they could be used to obtain information on tlie inner structure of superlattices. However, in tlie present study the smallness of these gaps ($< 1\text{cm}^{-1}$) hindered quantitative analyses. On the other hand, tlie relative intensities are very sensitive to tlie details of the structure, and can provide for the required additional data to deduce d_2/d. A calculation of the scattering efficiency is in progress to allow comparison with relative intensities already measured with $\lambda = 514.5$ nm excitation for the four different sets of d_2/d available.

Next, we consider the case of superlattices grown on Ge substrates, alternating $Ge/Ge_{0.7}Si_{0.3}$ layers of variou thicknesses. Tlie high resolution Raman spectra for representative samples are shown in Figs. 4 and 5. Nominal structural data are given at the right upper corner of tliese figures. The curves displayed in tliese figures differ greatly from those of tlie previously discussed samples. Instead of sharp lines the features are broad-bands either cut or intercalated by dips. These peculiar lineshapes arise both in the Stokes and anti-Stokes components of tlie spectra. These dips may arise by coupling between sharp phonon lines and a density of states-like features. A detailed study of selection rules and new measurements for different excitation wavelengths are needed for a better understanding in the subject.

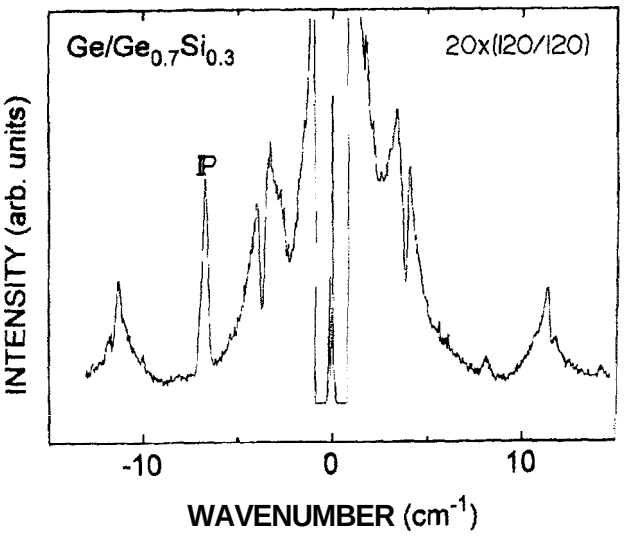

Figure 4: Raman spectrum of a sample grown on Ge-substrate using $\lambda = 514.5$ nm. Sampling depth $\sim$ 1.5 periods. P stands for a plasma line.

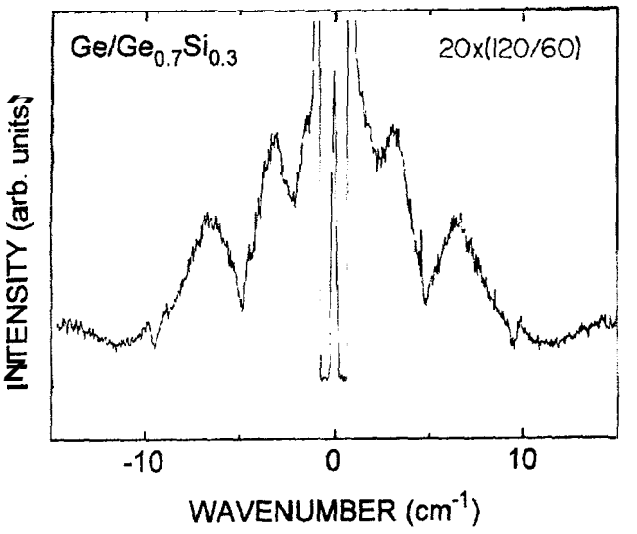

Figure 5: Raman spectrum of a sample grown on Ge-substrate using $\lambda = 514.5$ nm. Sampling depth $\sim$ 2 periods.

IV. Conclusion

High resolution Raman scattering measurement were performed for several Si/Ge_xSi_{1-x} superlattices, with different Ge composition and structural profile. A good estimate of the period was quickly obtained from tlie analysis of frequency shifts. The reliability of the method proved good in comparison with standard x-ray diffraction results. Detailed structural information

is also possible if a theoretical calculatioii on tlie relative intensities is provided. This is tlie aim for the sequence of this study. We also report on the observation of acoustic phonon spectra on $Ge/Ge_{0.7}Si_{0.3}$ superlattices of difèrent structural characteristics. For all of the samples the spectra display broad bands alternated with dips. The lineshapes and Stokes/anti-Stokes activity suggest phonon–phonon coupling as responsible for the observed profile. Further stuclies are necessary in order to understand these features better.

Acknowletlgments

We thanx professor F. Cerdeira for allowing the use of the samples, which were grown by J. C. Bean in AT&T Bell Labs (Murray Hill), and the student M. A. Araújo Silva for his help with the fittings. The financial support from CNPq and FAPESP is gratefully acknowledged.

References

1. B. Jusserand and RI. Cardona, in *Light scatteriny in solids V*, edited by M. Cardona and G. Güntherodt. *Topics in Applied Physics* 66 (Springer–Verlag, Berlin, 1989) p.49 and referentes therein.
2. D. J. Lockwood and J. F. Young, Light *Scattering in Semiconductor Structures and Superlattices* (Plenuin, New York, 1991).
3. V. Mazzacurati, P. Benassi and G. Ruocco, J. Phys. E: Sci. Instrum. **21**, 798 (1988).
4. D. J. Lockwood, M. W. C. Dharma–wardana, J. -M. Baribeau, and D.C. Houghton, Phys. Rev. B35, 2243 (1987).
5. R. Hull and J. C. Bean in *Semiconductors* and *Semimetals* vol.**33**, edited *by* T.P. Pearsall (Acad. Press, New York 1991) p.1.
6. V. S. Speriosu and T. Vreeland Jr., J. Appl. Phys. 56, 1591 (1984).
7. H. Brugger, H. Reiner, G. Abstreiter, H. Joike, H.J. Herzog and E. Kasper, Superlat. and Microstruct. 2, 451 (1986).
8. P. X. Zhang, D. J. Locltwood, H. J. Labbé and J. -M. Baribeau, Phys. Rev. B46, 9881 (1992).
9. P. X. Zhang, D. J. Lockwood and J. -M. Baribeau, Appl. Pliys. Lett. 62, 267 (1993).
10. S. M. Rytov, Sov. Phys. Acoust. **2**, 67 (1956).
11. J. Humlicek, M. Garriga, M. I. Alonso and M. Cardona, J. Appl. Phys. 65, 2827 (1989).
12. Landolt-Börnstein Tables, edited by O. Madelung, M. Shulz and H. Weiss (Springer, Berlin, 1984) Vol.**17b**.
13. B. Jusserand, D. Paquet, F. Mollot, F. Alexandre and G. le Roux, Phys. Rev. B35, 2808 (1987).